ÇUKUROVA UNIVERSITY
INSTITUTE OF NATURAL AND APPLIED SCIENCES

MSc THESIS

Mohammad WES

REGIONAL FLOOD FREQUENCY ANALYSIS OF THE FIRAT AND DİCLE BASINS IN TURKEY USING L-MOMENTS APPROACH AND PLOTTING-POSITION METHOD FOR MAXIMUM FLOW VALUES

DEPARTMENT OF CIVIL ENGINEERING

ADANA, 2021

ABSTRACT

MSc THESIS

REGIONAL FLOOD FREQUENCY ANALYSIS OF THE FIRAT AND DİCLE BASINS IN TURKEY USING L-MOMENTS APPROACH AND PLOTTING-POSITION METHOD FOR MAXIMUM FLOW VALUES

Mohammad WES

ÇUKUROVA UNIVERSITY
INSTITUTE OF NATURAL AND APPLIED SCIENCES
DEPARTMENT OF CIVIL ENGINEERING

Supervisor : Prof. Dr. Recep YURTAL
Year: 2021, Pages: 73
Jury : Prof. Dr. Recep YURTAL
: Prof. Dr. Neslihan SEÇKİN
: Prof. Dr. Mustafa DEMİRCİ

For the design of hydraulic structures such as dams, bridges, waterways, the maximum flood flow over the life of the project should be estimated. This peak value is estimated based on the values of the observed annual instantaneous maximum flow series. Several methods are used to estimate the maximum flow value, such as the L-moment and plotting position methods. Regional flood frequency analysis was performed in this study to the annual maximum flow series recorded previously in the Euphrates and Tigris basins in Turkey by using the L-moments method to estimate probability distribution parameters. The homogenous region was identified by using the L-moments method, and in different regions the Generalized Extreme Value, Generalized Normal, Generalized Pareto, Pearson Type 3, Generalized Logistic, and Wakeby distributions have been applied by using the Xtest software. The accuracy of the estimated quantiles is assessed through the regional L-moment algorithm. The extreme value distribution is found to be appropriate in the Fırat basin and normal distribution for Dicle basin in Turkey.

Key Words: Regional flood frequency analysis, L-moments, plotting-position , Fırat basin, Dicle basin.

ÖZ

YÜKSEK LİSANS TEZİ

TÜRKİYE'DE FIRAT VE DİCLE HAVZALARININ MAKSİMUM AKIŞ DEĞERLERİ İÇİN L-MOMENT YAKLAŞIMI VE NOKTALAMA-POZİSYON YÖNTEMİ İLE BÖLGESEL TAŞKIN FREKANS ANALİZİ

Mohammad WES

ÇUKUROVA ÜNİVERSİTESİ
FEN BİLİMLERİ ENSTİTÜSÜ
İNŞAAT MÜHENDİSLİĞİ ANABİLİM DALI

Danışman : Prof. Dr. Recep YURTAL
Yıl: 2021, Sayfa: 73
Jüri : Prof. Dr. Recep YURTAL
: Prof. Dr. Neslihan SEÇKİN
: Prof. Dr. Mustafa DEMİRCİ

Barajlar, köprüler, su yolları vb. gibi hidrolik yapıların tasarımı için proje ömrü boyunca maksimum taşkın debisini tahmin etmemiz gerekir. Bu pik değer, gözlemlenen yıllık anlık maksimum akış serilerinin değerlerine dayalı olarak tahmin edilmektedir. L-Moment ve Plotting Position yöntemleri gibi maksimum akış değerini tahmin etmek için kullanılan birkaç yöntem vardır. Bu çalışmada, olasılık dağılım parametrelerini tahmin etmek için Türkiye'de Fırat ve Dicle Havzalarında daha önce kaydedilen yıllık anlık maksimum akış serilerine L-momentler yöntemi kullanılarak bölgesel taşkın frekans analizi uygulanmıştır. Homojen bölgeler L-momentler yöntemi kullanılarak belirlenmiş ve farklı bölgelerde Xtest yazılımı kullanılarak Genelleştirilmiş Ekstrem Değer, Genelleştirilmiş Normal, Genelleştirilmiş Pareto, Pearson Tip 3, Genelleştirilmiş Logistic ve Wakeby dağılımları uygulanmıştır. Tahminlerin doğruluğu, bölgesel L-Moment algoritması ile değerlendirilmiştir. Sonuç olarak Türkiye'deki Fırat havzası için Ekstrem Değer dağılımın ve Dicle havzası için Normal dağılımın uygun olduğu görülmüştür.

Anahtar Kelimeler: Bölgesel taşkın frekans analizi**,** L-momentler, Noktalama Pozisyonu, First havzası, Dicle havzası

EXTENDED ABSTRACT

To design the hydraulic structures such as dams, water canals, and other facilities, we must determine the value of maximum flow in the canal during the life span of the project. This value is determined based on previous records for values of the maximum flows by using different methods to determine the maximum flow value, and the most famous method is L-moment.

This method was applied to the Dicle and Fırat basins. The values of the maximum flows were taken from records of previous years that were recorded in many stations within the two basins. The study was conducted as follows:

Dicle Basin

The study was conducted based on the flow values that were taken at 15 stations in previous years, and the homogeneity test was performed on all stations finding that the stations represent one homogeneous region. Performing Z test to determine the most appropriate distribution, The most appropriate distribution of the Dicle Basin was the normal distribution confirmed by performing the Z test, and subsequent estimation of maximum flows according to different frequencies.

The error value was calculated for different distributions, and the most appropriate distribution corresponding to the smaller error value between the error values. For Dicle Basin, the smallest error value is of the normal distribution ($\Delta nor=0,117$). In the last step, the relationship between area and flow values in the basin was found and represented by the appropriate curve.

Fırat Basin

The study was conducted on the basis of the flow values that were taken in previous years of 44 stations, and the homogeneity test was performed on all stations. Results show that they do not constitute one homogeneous region. Consequently, the

stations were divided into two groups and each of them forming a homogeneous region.

First Region

The first region consists of 28 stations, and a Z test was performed to determine the most appropriate distribution, and the most appropriate distribution was the extreme value distribution. According to the most appropriate distribution, maximum flow values were estimated according to different frequencies.

The error value was calculated for different distributions, and the most appropriate distribution corresponding to the smaller error value between the error values. For the first region of Fırat basin, the smallest error value is of the extreme value distribution (ΔGEV=0,031). In the last step, the relationship between area and flow values in the basin was found and represented by the appropriate curve.

Second Region

The second region consists of 16 stations, and a Z test was performed to determine the most appropriate distribution, and the most appropriate distribution was the extreme value distribution. According to the most appropriate distribution, maximum flow values were estimated according to different frequencies.

The error value was calculated for different distributions and the most appropriate distribution corresponding to the smaller error value between the error values. For the second region of Fırat basin, the smallest error value is of the extreme value distribution (ΔGEV=0,119). In the last step, the relationship between area and flow values in the basin was found and represented by the appropriate curve.

GENİŞLETİLMİŞ ÖZET

Barajlar, su kanalları ve diğer su yapılarını tasarlamak için, projenin ömrü boyunca gelebilecek maksimum su debisinin belirlenmesi gerekmektedir. Bu değeri tahmin etmek için geçmiş yıllara ait anlık maksimum debi değerleri kullanılır. Maksimum debi değerini belirlemek için farklı yöntemler önerilmiştir. Een çok kullanılan yöntem L-moment yöntemidir. Bu yöntem, iki havza içindeki birçok istasyonda önceki yıllara ait kaydedilen maksimum debi değerlerine uygulanmış ve çalışma aşağıdaki gibi yapılmıştır.

Dicle Havzası

Bu çalışmada, 15 istasyona ait önceki yıllarda ölçülen debi değerlerine göre tüm istasyonlar için homojenlik testi yapılmıştır. Sonuç olarak istasyonları bir homojen bölgenin temsil ettiği anlaşılmıştır. En uygun dağlımı belirlemek için Z Testi yapılmıştır. Dicle Havzası'nın en uygun dağılımı Genelleştirilmiş Normal Dağılım olarak bulunmuştur. En uygun dağılıma göre maksimum debi değerleri farklı frekanslara göre Tahmin edilmiştir.

Farklı dağılımlar için hata değeri hesaplanmıştır, Dicle Havzası için hata değerleri arasındaki en küçük hata değerine karşılık gelen dağlım en uygun dağılımdır. En küçük hata değeri Genelleşmiş Normal Dağılım'a ($\Delta GEV = 0{,}119$) aittir. Son adımda, havzadaki alan değerleri ile akış değerleri arasındaki ilişki bulunup, uygun eğri ile temsil edilmiştir.

Fırat Havzası

Bu çalışmada, 44 istasyona ait geçen yıllardaki ölçülen debi değerleri kullanılmış ve 44 istasyon için homojenlik testi yapılmıştır. Sonuç olarak istasyonları bir homojen bölgenin temsil etmediği gözlemlenmiştir ve istasyonların ayrı iki bölgeyi temsil etiği bulunmuştur.

Birinci Bölge

Birinci bölge 28 istasyondan oluşmaktadır ve en uygun dağılımı belirlemek için Z Testi yapılmıştır ve en uygun dağılımı Genelleştirilmiş Ekstrem Değer dağlımı göstermiştir. En uygun dağılıma göre, maksimum debi değerleri farklı frekanslara göre hesaplanmıştır. Son adımda, havzadaki alan değerleri ile debi değerleri arasındaki ilişki bulunmuş ve uygun eğri ile temsil edilmiştir.

Farklı dağılımlar için hata değeri hesaplanmıştır. Fırat havzası için hata değerleri arasındaki en küçük hata değerine (ΔGEV=0,031 karşılık gelen en uygun dağılım olarak Genelleşmiş Ekstrem Değer dağılımı bulunmuştur.

İkinci Bölge

İkinci bölge 16 istasyondan oluşmaktadır ve en uygun dağılımı belirlemek için Z Testi yapılmıştır ve en uygun dağılımı Genelleştirilmiş Ekstrem Değer dağlımı göstermiştir. En uygun dağılıma göre, maksimum debi değerleri farklı frekanslara göre hesaplanmıştır. Son adımda, havzadaki alan değerleri ile debi değerleri arasındaki ilişki bulunmuş ve uygun eğri ile temsil edilmiştir.

Farklı dağılımlar için hata değeri hesaplanmıştır, Fırat havzası için hata değerleri arasındaki en küçük hata değerine (ΔGEV=0,119) karşılık gelen en uygun dağılım olarak Genelleşmiş Ekstrem Değer dağılımı bulunmuştur.

ACKNOWLEDGEMENTS

First and foremost, I would like to express my appreciation to my supervisor, Prof. Dr. Recep Yurtal who has cheerfully answered my queries, provided me with materials, checked my examples, assisted me in a myriad way with the writing and helpfully commented on earlier drafts of this project. Also, I am also very grateful to my friends, family for their good humour and support throughout the production of this project.

And I would like to thank Prof. Dr. Neslihan SEÇKİN for standing by my side and providing assistance and support to me throughout the research preparation period.

CONTENTS **PAGE**

LIST OF TABLES **PAGE**

LIST OF FIGURES PAGE

ABBREVIATIONS

a_r : rth probability weighted moment of a frequency distribution.

B_r : rth probability weighted moment of a frequency distribution.

Cv : Coefficient of variation of a frequency distribution.

Di : Discordancy measure for site i in a region.

H : Heterogeneity measure for regional data.

K : Kurtosis of data sample.

lr : rth L-moment of a data sample.

S : Standard deviation of a data sample.

t : L-CV of a data sample.

tr : rth L-moment ratio of a data sample.

Var ( ) : Variance of a random variable.

Z : Goodness of fit measure for regional data.

μ : Mean of a frequency distribution.

1. INTRODUCTION

Rainstorms and sudden melting snow lead to flooding of watercourses damaging the environment around the watercourse. Recently, there have been many floods in Turkey that have caused great damage. In 1998, about 3,700 km^2 of land and more than 2 million people were affected by the Black Sea flood. In 2001, a rainstorm in Hatay triggered an unprecedented flood in the region.

The construction of hydraulic structures such as dams, artificial lakes, waterways, etc. should determine the value of the maximum flow during the life of the project (the design flow of the project). In this study, which will concentrate on the Fırat and Dicle basins, the two basins will be divided into homogeneous areas, and adopting the L-moment method will find the most appropriate distribution and the relationship through which the design flow can be estimated.

Planning and design of flood control now play an important role in the design of many hydraulic structures. Analysis of maximum precipitation and flows gained importance in such studies. While a maximum rainfall intensity of two and five years is needed for drainage studies to be designed in a residential area, maximum precipitation and flow values with a recurrence period of 25 years are required for erosion and sediment control studies, and 100 years for structures such as dams, ponds, and irrigation facilities. For this reason, the magnitude of the possible flood is estimated using statistical methods, based on the maximum annual flow values obtained from the flow observation stations established on the rivers by the State Hydraulic Works (DSI) and the Electricity Works Survey Administration (EIEI). The longer the observation times of the stations used in the analysis, the closer the estimated recurrence values will be to the correct values. Thus, the magnitude of the possible flood is predicted and measures are taken to minimize the damage.

In this study, regional frequency analysis was applied to the maximum annual flow values of 59 stations in the Tigris and Euphrates basins in Turkey using the L-moments technique to estimate the distribution parameters. As a

regionalization technique, the L-moment algorithm obtained using L-moments in the index flood method was used. Recurrence values were obtained by applying generalized normal (GNO), generalized extreme value (GEV), generalized logistic (GLO), generalized pareto, Pearson type 3 and Wakeby distributions to the homogeneous regions. The accuracy of the estimated recurrence values was obtained by Monte Carlo simulation. The analyses were performed by Hosking (2000) through sub-programs prepared at the IBM research center in the USA. These programs were run separately for each distribution, and the outputs were interpreted.

2. PREVIOUS STUDIES

In the study conducted by Anli (2007), to do the regional flood frequency estimation of Göksu River Basin in Turkey/Eastern Mediterranean Region, the L-moment technique was used. Annual maximum streamflow series of 10 years in the basin for 10 streamflow gauging stations were used. First, all the gauging stations were assumed as a region and regional analyses were performed. After assuming all the gauging stations as a region, a regional frequency analysis was utilized. Station 1723 value was discordant with the number of stations, which have a value greater than the critical value (2.49) was 10 in the observed flows at the station. The outlier value (1775 m^3/s) was removed, so discordancy measure became less than 2.49. The suggested region was accepted as a homogeneous region because the heterogeneity measure values were less than the critical value 1. Finally, regional flood frequency estimation was performed for different times.

Rao and Hamed (1997) conducted the Wabash basin regional flood frequency analysis using the L-moments technique. Heterogeneous as a single site, they geographically divided the Wabash Basin into four sub-regions. These regions' degrees of homogeneity were calculated using Wiltshire's homogeneity test and L-moment ratios. Pearson type 3, GEV, for homogeneous and heterogeneous regions GLO, log normal distributions and conformity tests and determined the most appropriate distributions at the point and regional level.

Seçkin (2009) estimated the probability distribution parameters for the annual flood peaks, which belong to 455 stations in 26 river basins in Turkey, applied the regional flood frequency analysis using the L-moments method to identify the homogenous region and used the index flood method based on L-moments method in different regions as well as applied the GEV, GNO, generalized pareto, Pearson type 3, GLO, and Wakeby distributions by using the Monte Carlo simulation. The accuracy of the estimated quantiles is assessed through the regional L-moment

algorithm. The GLO distribution is generally found to be suitable for river basins in Turkey.

Forty-two stations from the Fırat basin were included in the study. When the region is evaluated as a whole, stations 2123 and 2165 were found to be incompatible according to the critical D_i value. The basin was heterogeneous according to the heterogeneity test. Therefore, the basin EIE, hydrologically separated by the lower, middle, and upper Fırat, are evaluated in three sub-regions. In this way, heterogeneity test was conducted in three sub-regions and three regions were homogeneous. GEV, GNO distribution, and Pearson 3 distribution in the Middle Fırat basin; GLO in the Lower Fırat basin; GEV, GNO, and Generalized Pareto distributions, and GLO distribution in the Upper Fırat basin were found appropriate according to the results.

Fifteen stations from the Dicle basin were included in the study. There are no incompatible stations. According to the H values, the region is acceptably homogeneous. The Xtest software obtained the distribution of measurements. According to these results, GLO, GEV, and GNO distribution were found suitable for the region.

Peng et al. (2009) demonstrated that the low-flow analysis by L-moments in the Karst region in southwest China was in good agreement and that the logical probability distribution GLO was the most appropriate distribution. Shi et al. (2010) also applied L-moments for regional frequency analysis to examine low flow in the Karst area of southwest China. Their results indicated that, based on the L-moments ratio diagram Z^{DIST} and t_4 statistic criteria, GLO distribution was a robust distribution for the study area. Dodongeh et al. (2013) used L-moment for low-flow frequency analysis at ungauged sites in the Sefidroud basin of northwestern Iran.

Keshtkar (2015) employed a data set of 20 river flow time-series from the Iranian Central Plateau River Basin, Iran. The lowest residual sum of squares (RSS) values were used to select the best distribution for each station. The results showed that the L-moment method provided reasonably good accuracy for at-site as well as

ungauged site frequency analysis and that Pearson type 3 distributions were the best-fit regional model for the Iranian Central Plateau River Basin. Ahmad et al. (2017) examined regional frequency analysis of low flows using L-moments for Indus basin in Pakistan. They separated the region into two regions. GNO was found to be the most appropriate probability distribution for Region-I and GPA for Region-II.

Haktanir (1982) used plotting position formulas and probability distribution. He has developed a flood frequency analysis computer program covering models and short processing time with the option to select recurrence times from one to twenty and up to 10,000 years. This program can also determine the compatibility of the distribution models with the sample by performing a chi-squared (χ^2) and Kolmogorov-Smirnov fitness tests. With the help of this program, he applied seven distributions to the flood peak series of six flow observation stations in the Seyhan-Ceyhan basins and determined that the most appropriate distributions were log-gamma and log - normal distributions.

Hosking et al. (1985a), Lettenmaier and Potter (1985), Wallis and Wood (1985), Lettenmaier et al. (1987), Hosking and Wallis (1988), and Potter and Lettenmaier (1990) claimed that the indicator flood method based on L-moments or probability-weighted moments gives strong and accurate predictions. Numerous simulation studies have shown that "L-moments method", "Method of moments", "maximum likelihood method", "least squares method", "graphic method" and "probability weighted moments method" considering the root mean square errors of the estimations of the parameters, gives more approximate results than (Hosking and Wallis, 1987; Rosbjerg et al., 1992).

Özcan (1990) developed a computer model that has gained popularity in the hydrology literature of the last 10 years, calculating six different distribution models with two or three different parameter estimation methods and performing point flood frequency analysis. By applying this model to the annual flood peak series of 112 stations with a duration of 21 years and longer on 23 basins in Turkey's natural rivers,

it has been determined that the Log-Pearson 3 and Log-Logistic distributions show the best fit for these station data.

Muhara (2001) determined the regional statistical distributions and hydrologically homogeneous regions for stations in the Tanzania region in Kenya with the help of L-moments diagrams. The study performed a linear regression model for homogeneous regions and for the whole of Tanzania. Study results determined that the log-logistic distribution in 2 of the 12 regions in Tanzania, the generalized Pareto distribution in 1, the 3-parameter Log normal distribution in 4, and the Pearson type 3 distribution in 4 were suitable. Muhara determined that he did not have enough data for a region analysis, but when he examined Tanzania as a single region, the Pearson type 3 distribution fits the instantaneous annual maximum flows.

3. MATERIAL AND METHOD

3.1. Material

In this study, we will rely on the flow values of the previous years for stations located on the Dicle and Fırat rivers. Annual maximum flow values of the stations in the Dicle and Fırat basin in the current observational years of the Electricity Works Survey Administration and State Water Works were used as material (DSI, 1994).

3.1.1. Dicle Basin

Turkey is considered one of the richest countries with rivers. The Dicle river stems from Turkey and crosses Iraqi territory, as shown in Figure 3.1. The river gets its main resources from the mountains of the Eastern Anatolia Region and from the Caspian Lake near Elazig by infiltration from the bottom. The Dicle total length is 1900 km. The length of the river within Turkish territory is 523 km. Its most important branches are Batman and Yanarsu, Botan, Habur, Büyük Zap and Küçük Zap. Its flow rate is 360 m^3/sec on average, at its smallest with 55 m^3/s in mid-September, and its peak 2263 m^3/s at the end of February. The water generally decreases in the river due to drought in late summer and early autumn and lack of precipitation. Despite this, it swells with water which is formed by the melting of snow in late and early spring.

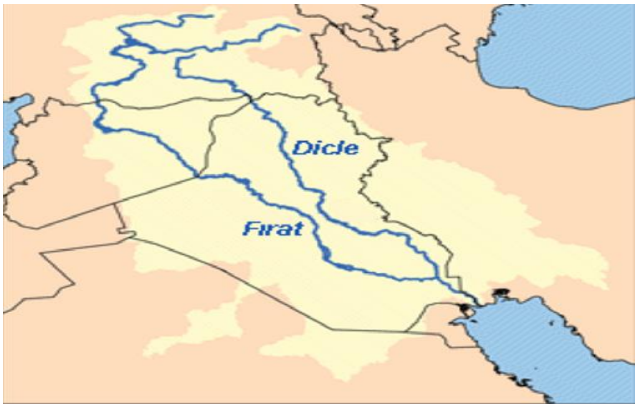

Figure 3.1. Dicle and Firat rivers

Annual maximum flow values of the stations in the Dicle Basin utilized two material resources. They include the current observational years of the Electricity Works Survey Administration (EIEI) and State Water Works (DSI) (DSI, 1994) (Table 3.1).

Table 3.1. Flow values of the stations in the Dicle basin

Station name	Duration of observation (Years)	Drainage Area (km^2)	Qmean (m^3/s)
2603	54	2450,4	577,7
2604	21	7628	915,0
2605B	21	5655,2	1325,2
2606	28	38280,7	3553,2
2610	49	640,4	210,0
2612	42	4105,2	1195,7
2617	25	1186	559,2
2618	29	976	225,6
2620	34	5344,4	312,4
2621	29	2504,4	65,8
2624	36	1169,6	253,7
2625	27	1127,2	193,4
2626	27	7989,2	524,1
26-024	17	1359,3	233,0
26-028	14	125,7	18,4

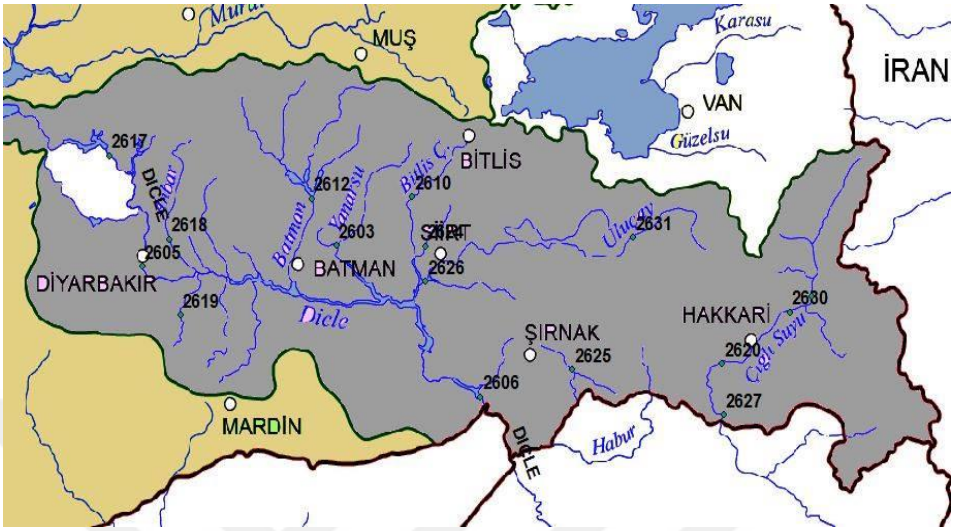

Figure 3.2. Used stations in Dicle basin

3.1.2. Fırat Basin

Fırat is the longest river in Southwest Asia. The starting points are the Murat River, stemming from Agri Diyadin, and the Karasu, stemming from Erzurum, Dumludag. These rivers merge in the Elazig province borders and form the Euphrates River. After determining the provincial border of Erzincan, Tunceli, Elazig, Malatya, Diyarbakır, Adiyaman, Gaziantep, Sanliurfa and Syria, the Fırat river then enters Iraqi territory. At a point that is not far from the sea in Iraq, it combines with the Dicle River and forms the Shatt'ul-Arab and pours into the Persian Gulf (Figure 3.1). Water year maximum flow values of the stations in the Fırat basin in the current observational years of the Electricity Works Survey Administration and State Water Works were used as material (DSI, 1994) (Table 3.2).

Table 3.2. Flow values of the stations in the Dicle basin

Station name	Duration of observation (Years)	Drainage Area (km^2)	Qmean (m^3/s)
21-001	26	233,2	22,1
21-019	27	303	25,8
21-026	20	128,4	6,2
21-041	22	2062	283,9
21-052	27	534	74,7
21-056	23	280	25
21-074	25	232	88,1
21-081	21	242,1	22,4
21-084	22	103,2	18,0
21-085	23	266,8	51,2
21-096	17	725,9	37,3
21-099	20	127,8	18,4
21-101	23	2047,8	36,8
21-103	22	136,1	27,9
21-116	22	222,4	33
21-132	18	271,6	22
21-133	17	463,7	57,5
2102	40	25447,2	1946,9
2103	45	63873,6	3416,1
2109	38	20687,6	948,1
2115	55	3990,4	515,1
2119	40	10356	477,8
2122	48	5882,4	543,3
2123/A	24	863,6	30,6
2124	54	1336,4	42,6
2131	60	277,6	30
2132	35	525,2	17,2
2133	48	3284,8	551,9
2141	27	3604,4	570,1
2145	54	5822	113,5
2147	42	807,6	170,7
2149	40	1622,4	318,1
2151	43	8185,6	455,1
2154	50	2886	173,4
2156	48	15562	675,8
2157	48	2098,4	263
2158	47	1577,6	281,1
2159	25	1036	121,6
2160	21	1020	61,2

Table 3.2. (Continued)

2164	47	2232	537,2
2165	29	490	61,1
2166	38	5446	718
2167	22	4288	342,8
2168	23	44	7

3.2. Method

3.2.1. L-Moment

L-moments are ameliorations over ordinary product moments and used to describe the type of a frequency distribution in addition to estimate the parameters of distribution, mostly for a small size of ecological data. For a more detailed description of L-moments, the reader can return to Hosking. The sample L- moments can be estimated by Equation 2.1:

$$\lambda r + 1 = \Sigma Pr.k * rk0.\beta k \quad (3.1)$$

Where

$$Pr, k = (-1)r - k.(rk).(r + kk) \quad (3.2)$$

It is appropriate to define dimensionless versions of L-moments.
This is achieved by dividing the higher - order L-moment by the scale measure $\lambda 2$.
We define the L-moment ratios using Equation 3.3.

$$\zeta r = \lambda r \lambda 2 \; r = 3{,}4 \quad (3.3)$$

The distribution independently of its scale of measurement can be measured using the L-moment ratios.

3.2.2. Plotting-Position Method

Probability-weighted moments of a random variable (X) with cumulative distribution function F( ) and quantile function x( ) were defined by Greenwood et al.(1979) to be the quantities

$$M_{p/s} = E\left(X^P\left(F(X)\right)^r\left(1-F(X)\right)^s\right) \quad (3.4)$$
$$= \int_0^1 \left(x(u)\right)^p u^r (1-u)^s \, du$$

Particularly, useful special cases are the probability-weighted moments

$$a_r = M_{1,0,r} = \int_0^1 (1-u)^r x(u) \, du \quad (3.5)$$

$$\beta_r = M_{1,r,0} = \int_0^1 u^r x(u) \, du \quad (3.6)$$

We can interpret a certain linear combination of probability weighted moments as measures of the location shape and scale of the probability distribution. This is how Hosking (1990) defined L- moments to be the quantities.

$$\lambda_r = \int_0^1 x(u) p_{r-1}^*(u) du \quad (3.7)$$

$$p_r^*(u) = \sum_{k=0}^r P_{r,k}^* . u^k \quad (3.8)$$

Where:

$$p_{r,k}^* = (-1)^{r-k}\binom{r}{k}\binom{r+k}{k} = \frac{(-1)^{r-k}(r+k)!}{(k!)^2(r-k)!} \quad (3.9)$$

L-moments are given in terms of the probability weighted moments by equation 3.10.:

$$\lambda_{r+1} = (-1)^r \sum_{k=0}^{r} p_{r,k}^{*}, a_k = \sum_{k=0}^{r} p_{r,k}^{*}, \beta_k \quad (3.10)$$

By dividing the higher-order L-moments by the scale measure we can achieve dimensionless versions of L-moments , L-moment ratios , r=3, 4, 5… are defined by equation 3.11.

$$\zeta_r = \frac{\lambda_r}{\lambda_2} \quad (3.11)$$

The shape of a distribution independently of its scale of measurement is measured by L-moment ratios.

The ratios ζ_3 (L skewness) and ζ_4 (L kurtosis) are used as measures of skewness and kurtosis, respecively.

Estimators:

there are two established ways of estimating the probability weighted moment a_r by giving an ordered sample of size n $x_{1:n} \leq x_{2:n} \leq \cdots \leq x_{n:n}$, Landwehr et al. (1979a) used the unbiased estimator.

$$a_r = n^{-1} \sum_{j=1}^{n} \frac{(n-j)(n-j-1)\ldots(n-j-r-1)}{(n-1)(n-2)\ldots(n-r)} x_{1:n} \quad (3.12)$$

Landwehr et al. (1979b) preferred the estimator

$$\bar{a}_r = n^{-1} \sum_{j=1}^{n} \left(1 - p_{j,n}\right)^r . x_{j,n} \quad (3.13)$$

While $p_{j:n} = (j - 0{,}35)/n$. And because $p_{j:n}$ is a plotting position, a distribution free estimator of the nonexceedance probability of $x_{j,n}$.We can call this a plotting-position estimator.

Estimator can similarly be obtained for the probability weighted moments β_r and L-moments and L-moment ratios. For L-moments, unbiased estimators are given by equation (3.14)

$$l_{r+1} = (-1)^r \sum_{k=0}^{r} P_{r,k}^{*} a_k \qquad (3.14)$$

The analogous estimators of L-moment ratios are

$$t_r = \frac{l_r}{l_2} \qquad (3.15)$$

These estimators are not exactly unbiased, but from their construction, it is suitable to refer to them as ‘unbiased’ estimators. Plotting-position estimators of L-moments and L-moment ratios are given by equation (3.16).

$$\bar{\lambda}_{r+1} = (-1)^r \sum_{k=0}^{r} p_{r,k}^{*}, a_k \qquad \bar{\zeta}_r = \frac{\bar{\lambda}_r}{\bar{\lambda}_2} \qquad (3.16)$$

Unbiased and plotting-position estimators are asymptotically equivalent in large samples: the difference between them is of stochastic order n^{-1}. The question of which is preferable in practice, therefore, depends on the estimators’ properties in small and moderate samples.

4. REGIONAL HOMOGENEITY TESTS

Regional frequency analysis consists of several stages. Homogeneous regions are considered the most difficult to identify. In the regional frequency analysis, a single frequency distribution is applied to the whole region. The region must be homogeneous and the homogeneity condition, which means that the same frequency distribution can be applied to the region other than the scale factor specific to each station, must be provided for this application.

The at-site frequency distributions are the same except for a site-specific scale factor; this is the hypothesis of homogeneity. If the data at the N sites in the region are consistent with this relation between the at-site frequency distribution, then we can conduct a test of the hypothesis of homogeneity. The test is most conveniently constructed as a statistical significance test of the similarity of appropriately chosen statistics calculated from the at-site data.

S test would be needed if the region were indeed homogeneous. S is then constructed the measures the difference between the at-site estimates and the regional estimate. One possible choice is S would have if the region were indeed homogeneous.

$$S = \sum_{i=1}^{N} \left(\hat{\theta}^{(i)} - \hat{\theta}^{R}\right)^2 \qquad (3.17)$$

Where:

θ a quantity that measures some aspect of the frequency distribution and is constant in a homogeneous region.

$\hat{\theta}^{(i)}$ is an at-site estimate based on the data for site i.

$\hat{\theta}^{R}$ is a regional estimate using data from all the sites in the region and assuming homogeneity.

4.1. Heterogeneity Measure (Formal Definition)

Lets assume that a region has N sites with the first site has value n_i with the sample L-moment ratios $t^i, t_3^i \; and \; t_4^i$. Denote by $t^R, t_3^R \; and \; t_4^R$ the regional average L-CV, L-skewness, and L-kurtosis, weighted proportionally to the sites record values.

$$t^R = \frac{\sum_{t=1}^{N} n_i t^{(i)}}{\sum_{i=1}^{N} n_i} \tag{4.1}$$

Then we calculate the weighted standard deviation of the at-site sample L-CVs

$$V = \left(\frac{\sum_{i=1}^{N} n_i \left(t^{(i)} - t^R\right)^2}{\sum_{i=1}^{N} n_i} \right)^{0,5} \tag{4.2}$$

For N values of V we can determine the mean and standard deviation of these values from the simulations

Then we Calculate the heterogeneity measure using equation 4.4 .

$$H = \frac{V - \mu_V}{\sigma_V} \tag{4.3}$$

If H is sufficiently large we can declare the region to be heterogeneous and if H<1 we can assume that the region to be regarded as ‘acceptably homogeneous’ , possibly heterogeneous’ if $1 \leq H \leq 2$ and if $H \geq 2$ we can say it is definitely heterogeneous’ .

5. USED DISTRIBUTIONS

5.1 Normal Distribution

It is well known that it conforms well to the normal distribution given in hydrology and many other disciplines. This can be explained by the central limit theorem. According to the central limit theorem, if a random variable (X) occurs in the sum of n independent variables, as n increases, the distribution of X rapidly approaches the normal distribution regardless of the distribution of the principal variables. In practice, this number can be assumed to be n = 10.

X is the probability density function of the normal random variable:

$$f(x) = \frac{1}{\sqrt{2\pi\sigma_x^2}} \exp\left[-\frac{1}{2}\left(\frac{x-\mu_x}{\sigma_x}\right)^2\right] \quad (5.1)$$

$$-\infty \leq x \leq +\infty$$

Average of distribution μ_x.

Variance $\sigma_x{}^2$.

The normal distribution is symmetrical, the coefficient of skewness is zero and the kurtosis is 3.

The two moments of distribution μ_x ve $\sigma_x{}^2$ are also the parameters.

L-moments of the distribution:

$$\lambda_1 = \mu \quad (5.2)$$

$$\lambda_2 = \frac{\sigma}{\sqrt{\pi}} \quad (5.3)$$

$$\lambda_3 = 0 \quad (5.4)$$

$$\lambda_4 = 0{,}1226 \quad (5.5)$$

Parameters of distribution:

$$\mu = \lambda_1 \qquad \sigma = \sqrt{\pi}.\lambda_2 \tag{5.6}$$

Since the additive distribution function of the normal distribution was not obtained analytically, it was tabulated by numerical integration. In order to prepare a uniform Table, the random variable was transformed into standard variable (z).

$$z = \frac{x-\mu_x}{\sigma_x} \tag{5.7}$$

Standard normal variable

$$\varphi(z) = 1 - 0{,}5\exp\left(-\frac{(83z+351)z+562}{\frac{703}{z}+165}\right) \tag{5.8}$$

The inverse form of the standard normal variable can be obtained approximately from the following expression.

$$\varphi^{-1}(p) = z_p = \frac{p^{0{,}135}-(1-p)^{0{,}135}}{0{,}1975} \tag{5.9}$$

A more precise approach $10^{-7} < p < 0{,}5$

$$\varphi^{-1}(p) = z_p = -\sqrt{\frac{y^2((4y+100)y+205)}{((2y+56)y+192)y+131}} \tag{5.10}$$

$y = -\ln(2p)$

The quantum corresponding to the probability of normal distribution and p is calculated by the following expression.

$$x_p = \mu_x + z_p . \sigma_x \quad (5.11)$$

5.2 Lognormal Distribution

If the Y variable defined by the logarithm of X is normally distributed, the distribution of X is lognormal. Since the distribution can be defined for X> 0, it fits well with many positive skewed variables in hydrology.

$$Y = \ln(X) \quad (5.12)$$

From the above equation, the actual X variable is passed with the following statement.

$$X = \exp(Y) \quad (5.13)$$

The additive distribution function of the lognormal variable X:

$$F(X) = p(X \leq x) = P(Y \leq \ln(x)) = P\left[\frac{Y - \mu_Y}{\sigma_Y} \leq \frac{\ln(X) - \mu_Y}{\sigma_x}\right]$$

$$= \varphi\left[\frac{\ln(X) - \mu_Y}{\sigma_Y}\right] \quad (5.14)$$

In the expression φ the standard is normal distribution. The following relationship exists between skewness and coefficient of variation in lognormal distribution.

$$C_{s_X} = 3C_{V_X} + {C_{V_X}}^3 \quad (5.15)$$

The lognormal distribution approaches the normal distribution as the skewness and coefficient of variation approach zero.

First two moments of lognormal distribution

$$\mu_X = \exp\left(\mu_Y + \frac{{\sigma_Y}^2}{2}\right) \quad (5.16)$$

$${\sigma_X}^2 = {\mu_X}^2[\exp({\sigma_Y}^2) - 1] \quad (5.17)$$

The relationship between the moments of the distributions of variable X and Y:

$$\sigma_Y = \left[\ln(1 + \frac{{\sigma_X}^2}{{\mu_X}^2})\right]^{0,5} \quad (5.18)$$

$$\mu_Y = \ln(\mu_X) - 0{,}5{\sigma_Y}^2 \quad (5.19)$$

In the last two equations, μ_Y and σ_Y can be calculated using the parameters of X.

The first two moments of the lognormal distribution, μ_Y and ${\sigma_Y}^2$, are taken by taking the logarithms of X_i values in Yi = ln (Xi).

In the following statement, using the denominator N-1 instead of N, the maximum likelihood estimation of the sample variance is obtained.

$${\sigma_X}^2 = \frac{\sum_0^N (X_i - \bar{X})^2}{N} \quad (5.20)$$

Estimating moments in this way is both easier and more effective. However, if there are very small values in the sample, the effect of these values on the sample is improved by logarithmic transformation.

Using equation (5.16) Second L moment of distribution can be calculate:

$$\lambda_2 = \exp\left(\mu_Y + \frac{{\sigma_Y}^2}{2}\right)\operatorname{erf}\frac{\sigma_Y}{2} = 2\exp\left(\mu_Y + \frac{{\sigma_Y}^2}{2}\right)\left(\varphi\left(\frac{\sigma_Y}{\sqrt{2}} - 0{,}5\right)\right) \quad (5.21)$$

Whether the expression applies to the 3-parameter lognormal.

XP quantified for a given probability P

$$X_P = \exp(\mu_Y + Z_P\sigma_Y) \quad (5.22)$$

The expression is determined.

GUMBEL DISTRIBUTION:

Gumbel's distribution function

$$f(x) = \frac{1}{a}\exp(-\frac{x-\xi}{a} - \exp(-\frac{x-\xi}{a})) \quad -\infty < x < +\infty \quad (5.23)$$

$$F(x) = \exp\left(-\exp\left(-\frac{x-\xi}{a}\right)\right)$$

a and ξ are the parameters of the distribution.

Mean, variance and skewness coefficient of the distribution:

$$\mu_X = \xi + 0{,}5772a \quad (5.24)$$

$${\sigma_X}^2 = \frac{\pi^2 a^2}{6} \quad (5.25)$$

$$C_{S_X} = 1{,}14 \quad (5.26)$$

L-moments of the distribution:

$$\lambda_1 = \xi + 0{,}5772a \quad (5.27)$$

$$\lambda_2 = a.\ln(2) \tag{5.28}$$

Moment's ratios:

$$\tau_1 = 0{,}1699 \tag{5.29}$$
$$\tau_2 = 0{,}1504$$

Estimation of the parameters of the distribution:

$$a = \frac{\lambda_2}{\ln(2)} = 1{,}443\lambda_2 \tag{5.30}$$

Or by the method of moments:

$$a = \frac{S_X\sqrt{6}}{\pi} = 0{,}7797S_X \tag{5.31}$$

$$\xi = \overline{X} - 0{,}5772a \tag{5.32}$$

The estimations made by the L-moments method are superior if the observations are indeed suiTable for the Gumbel distribution. The maximum likelihood method is superior to the quantitative estimates obtained with the most successful if the data shows a limited fit to the distribution.

5.3 Extreme Value Distribution

EVI (Gumbel) is a general distribution and includes II and III types together. GEV as shown in the literature and edf

$$F(X) = \exp\left(-\left(1 - \frac{k(X-\xi)}{a}\right)^{\frac{1}{k}}\right) \tag{5.33}$$

a, k and **ξ** are the parameters of the distribution; a is the scale parameter, k is the form parameter, and **ξ** is the ground parameter. For K = 0, the GEV distribution is EVI.

The general shape of the GEV distribution for | k | <0.3 is similar to the Gumbel distribution. The distribution for k> 0 is limited from the top. **ξ** + a / k is the upper limit and the distribution is called EVIII for this case. For k <0, the distribution is limited from the bottom. **ξ** + a / k is the lower limit and the distribution is called EVII.

Moments of distribution

The moments are given by Γ(.) Gamma function.

$$\mu_X = \xi + \left(\frac{a}{k}\right)\left(1 - \Gamma(1+k)\right) \tag{5.34}$$

$$\sigma_X^2 = \left(\frac{a}{k}\right)^2 \left(\Gamma(1+2k) - \left(\Gamma(1+k)\right)^2\right) \tag{5.35}$$

σ_X^2 is available for $k > -0{,}5$.

Skew:

$$C_{S_X} = \frac{-\Gamma(1+3k) + 3\Gamma(1+k)\Gamma(1+2k) - 2\Gamma^3(1+k)}{\left(\Gamma(1+2k) - \Gamma^2(1+k)\right)^{1{,}5}} \text{sign}(k) \tag{5.36}$$

Sign (k) indicates that the expression is multiplied by the sign of k.

Γ(.) The function can be obtained approximately from the following expression or can be calculated from the given Tables.

$0 \leq \delta \leq 1$ including

$$\Gamma(1+\delta) = 1 + \sum_{i=1}^{5} a_i \delta_i + \varepsilon \qquad (5.37)$$

$a_1 = -0{,}574865$

$a_2 = 0{,}951236$

$a_3 = -0{,}699859$

$a_4 = 0{,}424555$

$a_5 = -0{,}101068$

$|\varepsilon| \leq 5.10^{-5}$

In a simpler approach:

$$\Gamma(1+w) = w\Gamma(w) \qquad 0 < w < 1 \qquad (5.38)$$

For integers

$$\Gamma(1+w) = w!$$

L-moments of the distribution

$$\lambda_1 = \xi + \frac{a}{k}\left(1 - \Gamma(1+k)\right) \qquad (5.39)$$

$$\lambda_2 = \frac{a}{k}\left(1 - 2^{-k}\right)\Gamma(1+k) \qquad (5.40)$$

Moment ratios

$$\tau_3 = \left(\frac{2\left(1-3^{-k}\right)}{\left(1-2^{-k}\right)} - 3\right) \qquad (5.41)$$

$$\tau_4 = \frac{1-5(4^{-k})+10(3^{-k})-6(2^{-k})}{1-2^{-k}} \quad (5.42)$$

Estimation of the parameters of the distribution:

In L-moments

$$K=7.8590\ C+2.9554C2 \quad (5.43)$$

$$\text{The mean of the estimate is zero, variance } \mathrm{Var}(k) = \frac{0,5633}{N} \quad (5.44)$$

$$a = \frac{k\lambda_2}{\Gamma(1+k)(1-2^{-k})} \quad (5.45)$$

$$\xi = \lambda_1 + \frac{a}{k}(\Gamma(1+k)-1) \quad (5.46)$$

$$c = \frac{2\lambda_2}{\lambda_3+3\lambda_2} - \frac{\ln(2)}{\ln(3)} = \frac{2\beta_1-\beta_0}{3\beta_2-\beta_0} - \frac{\ln(2)}{\ln(3)} \quad (5.47)$$

For any probability P, the quantum can be found using the following expression:

$$X_P = \xi + \frac{a}{k}\left(1-\left(-\ln(F)\right)^k\right) \quad (5.48)$$

5.4 Pearson Type 3

Pearson type 3 distribution is frequently used in hydrology and especially in flood hydrology.

The distribution of:

$$f(X) = |\beta|\left(\beta(X-\xi)\right)^{a-1}\frac{exp(-\beta(X-\xi))}{\Gamma(a)} \quad (5.49)$$

a form of the distribution , β scale and **ξ** place parameter. For a> 0, β> 0, X> ξ **ξ** is the lower limit. For β <0, X <ξ, where **ξ** is the upper limit.

$$X > \xi \; için \; C_{S_X} = \frac{2}{\sqrt{a}} \; ve \; X < \xi \; için \; C_{S_X} = \frac{-2}{\sqrt{a}} \tag{5.50}$$

Furthermore, for β> 0 and ξ = 0, $C_{S_X} = 2CV_X$ is reduced to its distribution. In the case of a limit for constant mean and variance, a goes to infinity, skew goes to zero, and the Pearson type 3 distribution becomes a normal distribution. Again, a 2-parameter exponential distribution is obtained for a = 1 and $C_{S_X} = 2$.

Moments of distribution:

$$\mu_x = \xi + \frac{a}{\beta} \tag{5.51}$$

$$\sigma_x^2 = \tag{5.52}$$

L-moments of the distribution:

$$\lambda_1 = \xi + \frac{a}{\beta} \tag{5.53}$$

$$\lambda_2 = \frac{\Gamma(a+0{,}5)}{\sqrt{\pi}\beta\Gamma(a)} \tag{5.54}$$

Estimation of the parameters of the distribution:

By moments method

$$a = \frac{4}{C_{S_X}^2} \tag{5.55}$$

$$\beta = \frac{2}{\sigma_X C_{S_X}} \tag{5.56}$$

$$\xi = \mu_X - \frac{a}{\beta} = \mu_X - \frac{2\sigma_X}{C_{S_X}} \tag{5.57}$$

6. REGIONAL FLOOD FREQUENCY ANALYSIS

As all stations in a basin do not have the same climatic conditions and geographical characteristics, it is not correct to select the same flood frequency distribution. In order for the frequency analysis to give accurate results, the available hydrological data must be long enough. The available data on a station basis are often not sufficient. At the same time, as the available hydrological data have been measured by similar stations around that station, we have many data sets that are likely to have the same statistical characteristics for that data. With the analysis of the data at the relevant stations, the expectation is that more accurate results can be achieved if a new analysis technique called regional frequency analysis is conducted. Another important feature in the regional frequency analysis is that there is no requirement that the stations considered as a region be adjacent or close geographically (Şorman and Okur, 2000). A regional flood frequency analysis was used in this study. The region is divided into homogeneous sub-regions, provided that stations with similar statistical characteristics are considered for regional analysis. Thus, a general flood frequency distribution is obtained for each homogeneous region in flood estimates.

The indicator flood method, which is a regional frequency analysis method, is the principle that the frequency distributions in the stations considered as regions are the same except for a certain scale factor belonging to that station. As mentioned earlier, homogeneous basins belonging to stations considered as regions do not need to be geographically adjacent because geographic proximity does not require the same frequency distribution in the stations. This provides great advantages for regional frequency analysis, and stations can be regarded as a region without geographical proximity. Another advantage of this is that it reduces the correlation between stations.

7. INDICATOR FLOOD METHOD

The indicative method is a simple regionalization technique with a long history in hydrology and flood frequency analysis (Dalrymple, 1960). The indicative method is based on the separation of stations into homogeneous regions by assuming that the frequency distributions are the same except for the indicator flood, which is a scale factor of the stations.

$$Q_i(F) = \mu_i \, q$$

(F) represents the probability that F is not exceeded in the equation, μ_i the mean (index flood) at station i , and q(F) represents the same regional growth factor for each station. After obtaining the q(F) value as a result of the regional frequency analysis, multiplying this value with the average of the desired station and obtaining the $Q_i(F)$ value of the hydrological variable at the station to which F repeats. Assuming that in a region where there are N stations, i station is ni grain data and this data are symbolized as Q_{ij}, j = 1,2, …… ..n_i; q (F) = Q_{ij} / μ_i defined as the size of the common regional distribution of the function of the repetition function (quantile function) appears. The regional frequency analysis with the indicator flood method includes the following steps. Since L-moments and L-moment ratios are used in all of these stages, this state of the indicator flood method is called the regional L-moment algorithm (Hosking, & Wallis, 1997).

8. REVIEW OF DATA

The first rule of thumb in statistical analysis is to determine whether the available data are suitable for analysis. The non-compliance measure is used to review the data and to determine the compatibility of the stations considered homogeneous regions. The extent of mismatch depends on the number of stations in the region. A non-compliant station must be moved to another region or removed from the analysis. The mismatch measure is calculated using the L-moment ratios of the station data. The station's L-moment ratios (L-cv, L-skew, and L-kurtosis) are defined as the three-dimensional coordinates of a point. The L-cv and L-skewness values of these defined points form a group when mutually dotted in the graph, and this group has a center, that is, a midpoint. Any point called incompatible is quite far from this center. This distance criterion is defined as the correlation between sample L-moment ratios. The center of the set of points marked with (+) is the group average of L-cv and L-skewness values.

The ellipses having the same center with the small and large axes chosen for the data are calculated with the sample matrices of the L-moment ratios of the stations. Incompatible points are located outside the outermost ellipse. The vector form of L-moment ratios in a group of N stations is expressed as follows.

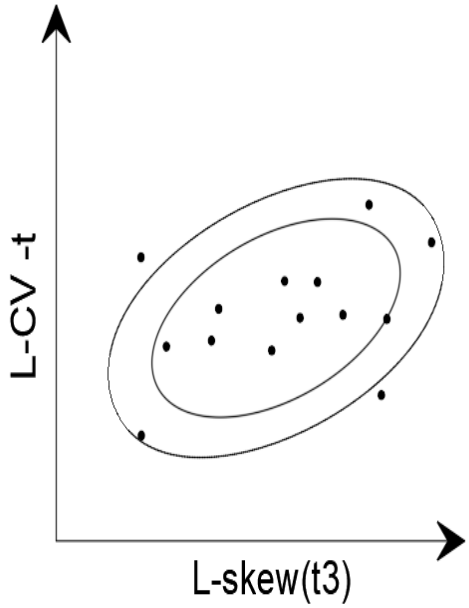

Figure 8.1. Relationship between L-Cv and L-Skewness values

Definition chart for incompatibility

$$U_i = \left(t^i, t_3^i, t_4^i\right)^T \tag{8.1}$$

T: Transposition of vector or matrix

$$\overline{U} = N^{-1} \sum_{i=1}^{N} U_i \tag{8.2}$$

$\overline{U}$: Weightless group average

$$A = \sum_{i=1}^{N} (U_i - \overline{U})(U_i - \overline{U})^T \tag{8.3}$$

A: Matrix of the sum of the squares and the cross product

$$D_i = \frac{1}{3} N (U_i - \bar{U})^T A^{-1} (U_i - \bar{U}) \quad (8.4)$$

D_i: Incompatibility measure for i station

D_i depending on the number of stations in the region. If the calculated Di value is greater than the critical Di value given in Table 8.1 that station is called incompatible.

Table 8.1. Di critical values (Source: Hosking And Wallis, 1997)

Number of stations in the region	Critical value	Number of stations in the region	Critical value
5	1.333	11	2.632
6	1.648	12	2.757
7	1.917	13	2.869
8	2.140	14	2.971
9	2.329	≥ 15	3.000
10	2.491		

9. USED SOFTWARE

In this study, Xtest software is used to find repetition values corresponding to a specific rotation range for frequency analysis known as the Return range. The software also calculates the discrepancy measure (Di) for each station, heterogeneity measure (H), and the suitability of the distribution (Z) for five distributions that are candidates for the region frequency distribution. This is achieved by applying a distribution to the region using L-moment algorithm, as well as building a simulation of the region to find the error value.

10. STUDY AND DISCUSS THE RESULTS

This study relied upon the values of maximum flows of the Dicle and Fırat rivers, which were obtained by the Electricity Directorate and the Water Corporation. The values of the flows were taken at stations that contain records for 10 years or more.

The study was conducted as follows:

- Conducting the homogenization test on the basin and divide it into homogeneous regions.
- Taking a test for each region and choose the most appropriate distribution for each region**.**
- Calculating the special constants for each distribution and determine the relationship by which to estimate the maximum flow of any area in the basin.

10.1 Dicle Basin

Values belonging to 12 stations were used in this study, As shown in the Table 10.1.

Table 10.1. Used stations in Dicle basin

Station name	Duration of observation (Years)	Drainage Area (km^2)	Qmean (m^3/s)
2603	54	2450,4	577,7
2604	21	7628	915,0
2605B	21	5655,2	1325,2
2606	28	38280,7	3553,2
2610	49	640,4	210,0
2612	42	4105,2	1195,7
2617	25	1186	559,2
2618	29	976	225,6
2620	34	5344,4	312,4
2621	29	2504,4	65,8
2624	36	1169,6	253,7

Table 10.1. (Continued)

2625	27	1127,2	193,4
2626	27	7989,2	524,1
26-024	17	1359,3	233,0
26-028	14	125,7	18,4

L-Moment Values were calculated using a plotting-position method usig Excel and the results are shown in Table 10.2.

Table 10.2. L-Moment values for Dicle Basin

Station name	Duration of observation (Years)	Qmean (m^3/s)	ζ_1	ζ_3	ζ_4	ζ_5	Di
D26-028	14	18,43	0,2977	0,3882	0,3768	0,1558	1,77
D26-024	17	233,00	0,2381	0,5298	0,4260	0,1267	**2,74**
D2626	27	974,41	0,2738	0,1874	0,0549	0,0476	1,27
D2625	27	193,43	0,2728	0,2099	0,1022	0,0436	0,54
D2624	36	253,69	0,2882	0,1862	0,1565	0,0496	0,34
D2621	29	65,81	0,2884	0,2861	0,1941	0,1264	0,09
D2620	34	312,44	0,2698	0,3804	0,2795	0,1245	0,6
D2618	29	225,58	0,3791	0,2456	0,1836	0,1092	1,46
D2617	25	559,24	0,3810	0,3840	0,2458	0,1234	2,11
D2612	42	1195,71	0,2807	0,1673	0,0895	0,0532	0,31
D2610	49	209,98	0,2723	0,1718	0,0701	0,0272	0,66
D2606	28	3553,18	0,2775	0,1272	0,1307	0,0902	1,12
D2605B	21	1325,19	0,3513	0,2267	0,1516	0,0601	0,66
D2604	21	914,97	0,2975	0,1731	0,1399	0,0332	0,35
D2603	54	577,72	0,2431	0,1584	0,1413	0,0498	0,97

An incompatibility measure was conducting finding that all values of D for all stations are less than a critical value (Dcr=3). This means that all stations are compatible with each other.

The following results were obtained using the Xtest software.

Table 10.3. The results of analysis for Dicle Basin

***** HETEROGENEITY MEASURES ***** (NUMBER OF SIMULATIONS = 500)	
OBSERVED S.D. OF GROUP L-CV	0,0403
SIM. MEAN OF S.D. OF GROUP L-CV	0,0355
SIM. S.D. OF S.D. OF GROUP L-CV	0,0066
STANDARDIZED TEST VALUE H(1)	0,72
OBSERVED AVE. OF L-CV / L-SKEW DISTANCE	0,0904
SIM. MEAN OF AVE. L-CV / L-SKEW DISTANCE	0,0813
SIM. S.D. OF AVE. L-CV / L-SKEW DISTANCE	0,0140
STANDARDIZED TEST VALUE H(2)	0,65
OBSERVED AVE. OF L-SKEW/L-KURT DISTANCE	0,1076
SIM. MEAN OF AVE. L-SKEW/L-KURT DISTANCE	0,1016
SIM. S.D. OF AVE. L-SKEW/L-KURT DISTANCE	0,0166
STANDARDIZED TEST VALUE H(3)	0,36

Depending on the previous H values, the region can be considered a homogeneous region. By performing a Z test, the most appropriate distribution of values can be obtained and the results are shown in Table 10.4.

Table 10.4. Z test's results for Dicle basin

DISTRIBUTION	**L-Kurtosis**	**Z**
Gen. Logistic	0,212	2,14
Gen. Extreme Value	0,178	0,54 *
Gen. Normal	0,165	-0,06 *
Pearson Type 3	0,142	-1,19 *
Gen. Pareto	0,097	-3,29

According to the values of Z, the most appropriate distribution is the one that has $|z|$ value closest to zero value. This indicates that GNO distribution is most appropriate. In general, all distributions that have $|z| < 1.64$ are appropriate.

Regional growth curve is derived based on the simulation results and the index flood procedure. Figure 10.1 shows the curve is fitting very well to his respective set of pooled flood peaks series in the region. Based on the distribution chosen by the goodness-of-fit test, we can see that the respective curve is also fitted statistically.

Table 10.5. Parameter estimates for distributions accepted at the 90% level for Dicle basin

DISTRIBUTI-ON	**ξ(Location Parameter**	**a(Scale Parameter**	**K(Shape Parameter**		
Gen. Extreme Value	0,742	0,379	-0,097		
Gen. Normal	0,881	0,465	-0,484		
Pearson Type3	1,000	0,545	1,408		
-------	ξ	a	B	γ	δ
Wakeby	0,234	1,780	6,789	0,56	-0,042

Repetitive function of the common regional probability distribution adapted to dimensionless data against certain rotation periods according to these parameters (quantile function) is shown in Table 10.6. The observed values and the flood frequency curves obtained from the distributions given in Table 10.6 were determined graphically (Figure 10.1).

Table 10.6. Quantile function for Dicle basin

Y	T	F	GEV	GNO	Observed Values
-0,8340	**1,1111**	0,1000	0,438	0,328	0,399
-0,4759	**1,25**	0,2000	0,566	0,547	0,560
0,3665	**2**	0,5000	0,883	0,993	0,925
1,4999	**5**	0,8000	1,354	1,456	1,384
2,2504	**10**	0,9000	1,695	1,691	1,667
2,9702	**20**	0,9500	2,047	1,872	1,924
4,6001	**100**	0,9900	2,939	2,168	2,451
5,2958	**200**	0,9950	3,365	2,265	2,653
6,9073	**1000**	0,9990	4,470	2,473	3,068
9,2103	**10000**	0,9999	6,382	2,887	3,531

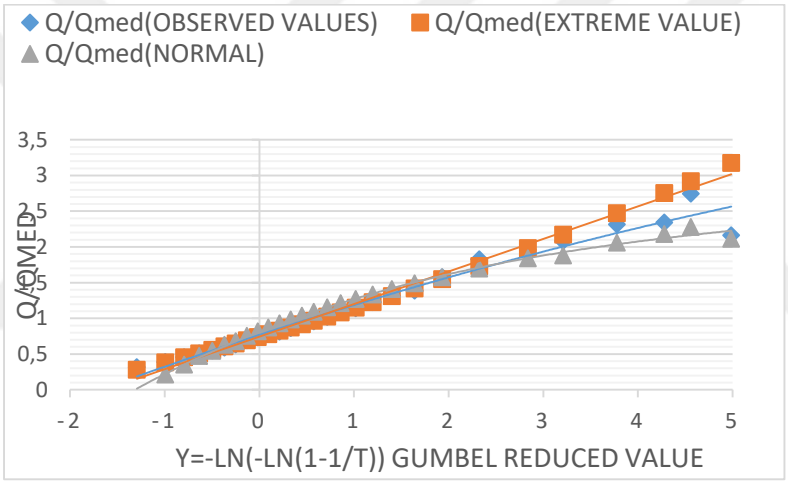

Figure 10.1. Flood frequency curves of Dicle basin

The error value was calculated for each distribution using equation 10.1. and finding the average value of the error values as shown in Table 10.7:

$$\Delta = \left|\frac{q - q_{obs}}{q_{obs}}\right| \qquad (10.1)$$

Table 10.7. The error values of each distribution for Dicle basin

Y	T	F	GEV	GNO	Observed Values	ΔGEV	ΔGNO
-0,834	**1,1111**	0,1	0,438	0,328	0,399	0,089	0,216
-0,4759	**1,25**	0,2	0,566	0,547	0,56	0,011	0,024
0,3665	**2**	0,5	0,883	0,993	0,925	0,048	0,068
1,4999	**5**	0,8	1,354	1,456	1,384	0,022	0,049
2,2504	**10**	0,9	1,695	1,691	1,667	0,017	0,014
2,9702	**20**	0,95	2,047	1,872	1,924	0,060	0,028
4,6001	**100**	0,99	2,939	2,168	2,451	0,166	0,131
5,2958	**200**	0,995	3,365	2,265	2,653	0,212	0,171
6,9073	**1000**	0,999	4,47	2,473	3,068	0,314	0,241
9,2103	**10000**	0,9999	6,382	2,887	3,531	0,447	0,223
					MEAN	**0,138**	**0,117**

According to the previous results, we find that the most appropriate distribution is the normal distribution. This was previously achieved according to the Z test.

The figure 10.2 shows the relationship between Y and the error values for each of the distributions.

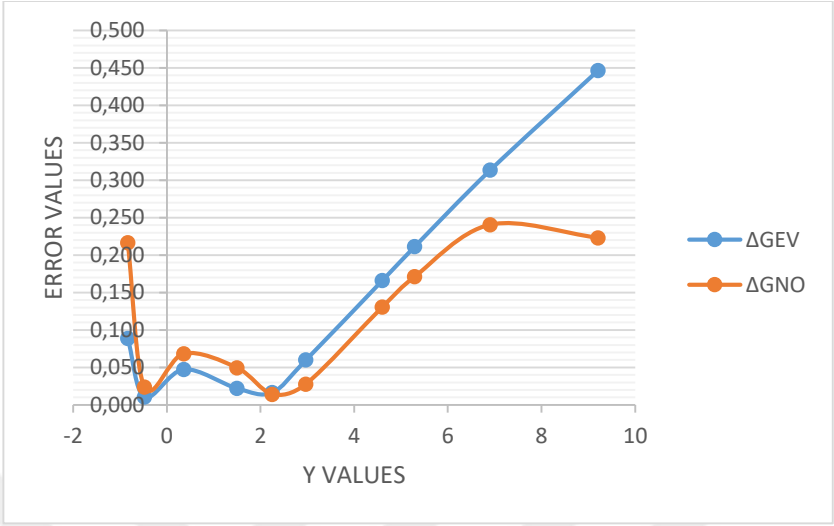

Figure 10.2. Relationship between y and the error values for each of the distributions

Flow values in the Dicle basin can be calculated using the relationship between area and flow using equation 10.2:

$$Q = 0{,}633A^{0{,}8407} \quad (10.2)$$

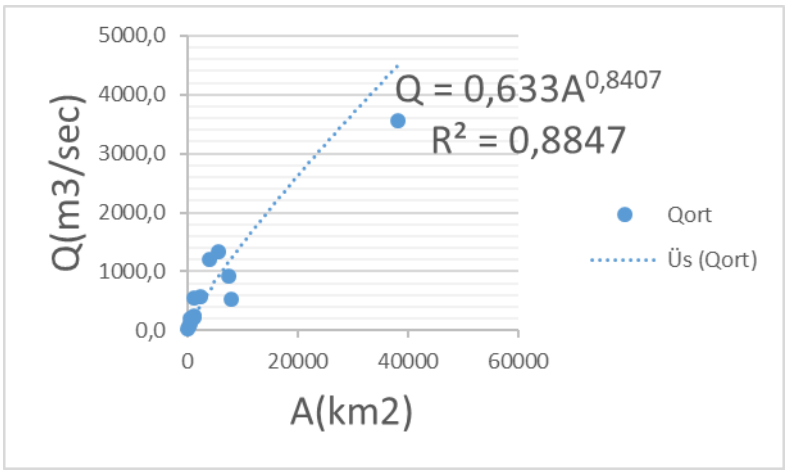

Figure 10.3. Relationship between area and flow for Dicle basin

The optimal distribution for the Dicle basin is the lowest absolute Z value, GNO has the lowest absolute z value. Using this distribution, regions were simulated 500 times with Monte Carlo simulation method (NSIM = 500) for GNO and GEV distribution. The dimensionless region growth rates, average errors, and errors of these rates bounds are given in Tables 10.8 and 10.9.

Table 10.8. Accuracy measures of the regional growth curve for Dicle basin (GNO).

T(Year)	F	q(F)	RMSE	Error bounds		
				95%	5%	Difference
1.11111	0.1	0.836	0.463	0.621	1.215	0.594
1.25	0.2	0.570	0.210	0.435	0.758	0.323
2	0.500	0.896	0.048	0.829	0.958	0.129
5	0.800	1.361	0.033	1.300	1.419	0.119
10	0.900	1.686	0.047	1.596	1.800	0.204
20	0.950	2.011	0.065	1.857	2.225	0.368
100	0.990	2.799	0.112	2.403	3.386	0.983
200	0.995	3.159	0.134	2.644	3.968	1.324
1000	0.999	4.051	0.190	3.108	5.587	2.479
10000	0.9999	5.478	0.281	3.668	8.654	4.986

Table 10.9. Accuracy measures of the regional growth curve for Dicle basin (GEV)

T(Year)	F	q(F)	RMSE	Error bounds		
				95%	5%	Difference
1.11111	0.1	0.438	0.526	0.250	0.921	0.671
1.25	0.2	0.566	0.159	0.458	0.720	0.262
2	0.500	0.883	0.055	0.806	0.953	0.147
5	0.800	1.353	0.049	1.290	1.406	0.116
10	0.900	1.693	0.034	1.615	1.779	0.164
20	0.950	2.044	0.052	1.907	2.228	0.321
100	0.990	2.934	0.11	2.532	3.552	1.020
200	0.995	3.359	0.139	2.799	4.279	1.480
1000	0.999	4.46	0.210	3.372	6.464	3.092
10000	0.9999	6.363	0.330	4.186	11.261	7.075

10.2 Fırat Basin

Values belonging to 40 stations were used in this study, as shown in the Table 10.10.

Table 10.10. Used stations in Firat basin

Station name	Duration of observation (Years)	Drainage Area (km^2)	Qmean (m^3/s)
F2168	23	44	7
F2166	38	5446	718
F2164	47	2232	537,2
F2158	47	1577,6	281,1
F2157	39	2098,4	263
F2156	48	15562	675,8
F2154	50	2886	173,4
F2151	43	8185,6	455,1
F2149	40	1622,4	318,1
F2147	42	807,6	170,7
F2145	54	5822	113,5

Table 10.10. (Continued)

F2141	27	3604,4	570,1
F2133	48	3284,8	551,9
F2124	54	1336,4	42,6
F2122	48	5882,4	543,3
F2119	40	10356	477,8
F2109	38	20687,6	948,1
F2103	45	63873,6	3416,1
F2102	40	25447,2	1946,9
F21-132	18	271,6	22
F21-116	22	222,4	33
F21-099	20	127,8	18,4
F21-084	22	103,2	18
F21-001	26	233,2	22,1
F21-041	22	2062	283,9
F21-052	27	534	74,7
F21-056	23	280	25
F21-074	25	232	88,1
F2167	22	4288	342,8
F2165	29	490	61,1
F2160	21	1020	61,2
F2159	25	1036	121,6
F2131	60	277,6	30
F2115	55	3990,4	515,1
F21-133	17	463,7	57,5
F21-103	22	136,1	27,9
F21-101	23	2047,8	36,8
F21-096	17	725,9	37,3
F21-085	23	266,8	51,2
F21-026	20	128,4	6,2

Table 10.11. The results of analysis for Firat basin

***** HETEROGENEITY MEASURES ***** (NUMBER OF SIMULATIONS = 500)	
OBSERVED S.D. OF GROUP L-CV	0,0995
SIM. MEAN OF S.D. OF GROUP L-CV	0,0391
SIM. S.D. OF S.D. OF GROUP L-CV	0,0045
STANDARDIZED TEST VALUE H(1)	13,31
OBSERVED AVE. OF L-CV / L-SKEW DISTANCE	0,1448
SIM. MEAN OF AVE. L-CV / L-SKEW DISTANCE	0,0884
SIM. S.D. OF AVE. L-CV / L-SKEW DISTANCE	0,0098
STANDARDIZED TEST VALUE H(2)	5,74
OBSERVED AVE. OF L-SKEW/L-KURT DISTANCE	0,1450
SIM. MEAN OF AVE. L-SKEW/L-KURT DISTANCE	0,1085
SIM. S.D. OF AVE. L-SKEW/L-KURT DISTANCE	0,0116
STANDARDIZED TEST VALUE H(3)	3,13

After conducting the analysis, it was found that the Fırat does not constitute a single homogeneous region, and therefore the region was divided into two homogeneous regions first and second Fırat.

10.2.1 First Region

Table 10.12. Used values in Firat basin for first region

Station name	Duration of observation (Years)	Drainage Area (km^2)	Qmean (m^3/s)
F2168	23	44	7
F2166	38	5446	718
F2164	47	2232	537,2
F2158	47	1577,6	281,1
F2157	39	2098,4	263
F2156	48	15562	675,8

F2154	50	2886	173,4
F2151	43	8185,6	455,1
F2149	40	1622,4	318,1
F2147	42	807,6	170,7
F2145	54	5822	113,5
F2141	27	3604,4	570,1
F2133	48	3284,8	551,9
F2124	54	1336,4	42,6
F2122	48	5882,4	543,3
F2119	40	10356	477,8
F2109	38	20687,6	948,1
F2103	45	63873,6	3416,1
F2102	40	25447,2	1946,9
F21-132	18	271,6	22
F21-116	22	222,4	33
F21-099	20	127,8	18,4
F21-084	22	103,2	18
F21-001	26	233,2	22,1
F21-041	22	2062	283,9
F21-052	27	534	74,7
F21-056	23	280	25
F21-074	25	232	88,1

L-Moment Values were calculated using a plotting-position method usig Excel and the results are shown in Table 10.13.

Table 10.13. L-Moment values for first region in Firat basin

Station name	Duration of observation (Year)	Q_{mean}	ζ_1	ζ_3	ζ_4	ζ_5	Di
F2168	23	6,97	0,1819	0,2618	0,2409	0,1199	2,8
F2166	38	717,97	0,2468	0,1904	0,1724	0,0122	0,03
F2164	47	537,21	0,2533	0,1218	0,1008	0,0467	0,49
F2158	47	281,06	0,3057	0,3143	0,2007	0,0686	1,82
F2157	48	263,03	0,2667	0,0586	0,0058	-0,0010	2,26
F2156	48	675,77	0,1993	0,1042	0,1340	0,0488	0,65
F2154	50	173,40	0,2170	0,1891	0,1378	0,0583	1,23
F2151	43	455,07	0,2282	0,1476	0,1307	0,0910	0,26
F2149	40	318,11	0,2322	0,1055	0,1795	0,0768	1,29
F2147	42	170,72	0,2202	0,2083	0,2656	0,1646	0,91
F2145	54	113,54	0,2983	0,2563	0,2363	0,1578	2,22
F2124	54	42,63	0,2909	0,1369	0,0961	0,0540	1,52
F2122	48	543,25	0,2096	0,1474	0,1726	0,0294	0,24
F2119	40	477,81	0,2217	0,1766	0,1738	0,0930	0,12
F2109	38	948,05	0,2098	0,1636	0,2129	0,0552	0,39
F2103	45	3416,12	0,2233	0,0571	0,0881	0,0624	0,91
F2102	40	1946,88	0,2133	0,1146	0,1255	0,0539	0,42
F21-132	18	22,04	0,2074	0,0937	0,1487	0,0081	0,57
F21-116	22	32,95	0,2500	0,2469	0,2550	0,0518	0,68
F21-099	20	18,37	0,1871	0,1779	0,2803	0,0904	1,75
F21-084	22	17,99	0,2226	0,1448	0,1501	0,1196	0,13
F21-001	26	22,12	0,2340	0,2215	0,1962	-0,0111	0,17
F21-041	22	283,86	0,2698	0,3367	0,2981	0,1596	1,65
F21-052	27	74,74	0,2495	0,3496	0,2841	0,1262	1,72
F21-056	23	24,99	0,2825	0,1933	0,1223	0,0335	0,78
F21-074	25	88,08	0,2794	0,2708	0,1465	0,0730	1,59

An incompatibility measure was conducting finding that all values of D for all stations are less than a critical value (Dcr=3). This means that all stations are compatible with each other.

The following results were obtained using the XTest software.

Table 10.14. The results of analysis for first region of Firat basin

***** HETEROGENEITY MEASURES ***** (NUMBER OF SIMULATIONS = 500)	
OBSERVED S.D. OF GROUP L-CV	0,0337
SIM. MEAN OF S.D. OF GROUP L-CV	0,0297
SIM. S.D. OF S.D. OF GROUP L-CV	0,0044
STANDARDIZED TEST VALUE H(1)	0,92
OBSERVED AVE. OF L-CV / L-SKEW DISTANCE	0,0698
SIM. MEAN OF AVE. L-CV / L-SKEW DISTANCE	0,0761
SIM. S.D. OF AVE. L-CV / L-SKEW DISTANCE	0,0099
STANDARDIZED TEST VALUE H(2)	-0,64
OBSERVED AVE. OF L-SKEW/L-KURT DISTANCE	0,0846
SIM. MEAN OF AVE. L-SKEW/L-KURT DISTANCE	0,0948
SIM. S.D. OF AVE. L-SKEW/L-KURT DISTANCE	0,0112
STANDARDIZED TEST VALUE H(3)	-0,91

Depending on the previous H values, the region can be considered a homogeneous region. By performing a Z test, the most appropriate distribution of values can be obtained and the results are shown in the Table 10.15.

Table 10.15. Z test's results for first region of Firat basin

DISTRIBUTION	**L-Kurtosis**	**Z**
Gen. Logistic	0,212	1,61*
Gen. Extreme Value	0,178	-1,50*
Gen. Normal	0,165	-1,90
Pearson Type 3	0,142	-2,98
Gen. Pareto	0,097	-8,34

According to the values of Z, the most appropriate distribution is the one that has $|z|$ value closest to zero value. This indicates that GEV distribution is most appropriate. In general, all distributions that have $|z| < 1.64$ are appropriate.

Regional growth curve is derived based on the simulation results and the index flood procedure. Figure 10.4 shows the curve is fitting very well to his respective set of pooled flood peaks series in the region. Based on the distribution chosen by the goodness-of-fit test, we can see that the respective curve is also fitted statistically.

Table 10.16. Parameter estimates for distributions accepted at the 90% level for first region of Firat basin

DISTRIBUTION	ξ (Location Parameter)	a (Scale Parameter)	K (Shape Parameter)
Gen. Logistic	0,933	0,227	-0,173
Gen. Extreme Value	0,800	0,343	-0,005

Repetitive function of the common regional probability distribution adapted to dimensionless data against certain rotation periods according to these parameters (quantile function) is shown in (Table 10.16). The observed values and the flood frequency curves obtained from the distributions given in Table 10.17 were determined graphically (Figure 10.14).

Table 10.17. Quantile function for first region of Firat basin

Y	T	F	GLO	GEV	Observed Values
-0,8340	**1,1111**	0,1000	0,518	0,501	0,428
-0,4759	**1,25**	0,2000	0,653	0,637	0,618
0,3665	**2**	0,5000	0,933	0,926	0,918
1,4999	**5**	0,8000	1,289	1,317	1,32
2,2504	**10**	0,9000	1,540	1,576	1,587
2,9702	**20**	0,9500	1,896	1,906	1,842
4,6001	**100**	0,9900	2,529	2,397	2,421
5,2958	**200**	0,9950	2,903	2,642	2,668
6,9073	**1000**	0,9990	3,962	3,213	3,241
9,2103	**10000**	0,9999	3,98	4,063	4,059

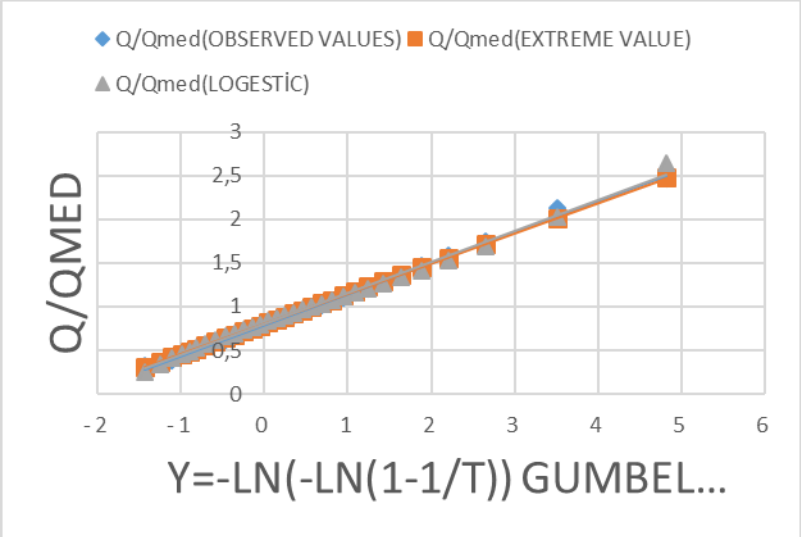

Figure 10.4. Flood frequency curves for first region of Fırat basin

Flow values in the first region of Fırat basin can be calculated using the extreme value relationship 10.3:

$$q = 0{,}8 - 68{,}6 * \left(1 - (-ln(F)^{-0{,}005})\right) \qquad (10.3)$$

The error value was calculated for each distribution using equation 10.1 and finding the average value of the error values as shown in Table 10.18:

Table 10.18. The error values of each distribution for first region of Firat basin

Y	T	F	GLO	GEV	Observed Values	∆GLO	∆GEV
-0,834	**1,1111**	0,1	0,518	0,501	0,428	0,174	0,146
-0,476	**1,25**	0,2	0,653	0,637	0,618	0,054	0,030
0,3665	**2**	0,5	0,933	0,926	0,918	0,016	0,009
1,4999	**5**	0,8	1,289	1,317	1,32	0,024	0,002
2,2504	**10**	0,9	1,54	1,576	1,587	0,031	0,007
2,9702	**20**	0,95	1,896	1,906	1,842	0,028	0,034
4,6001	**100**	0,99	2,529	2,397	2,421	0,043	0,010
5,2958	**200**	0,995	2,903	2,642	2,668	0,081	0,010
6,9073	**1000**	0,999	3,962	3,213	3,241	0,182	0,009
9,2103	**10000**	0,9999	3,98	4,063	4,059	0,020	0,001
					Mean	**0,056**	**0,031**

According to the previous results, we find that the most appropriate distribution is the extreme value distribution. This was previously achieved according to the Z test.

The figure 10.5 shows the relationship between Y and the error values for each of the distributions.

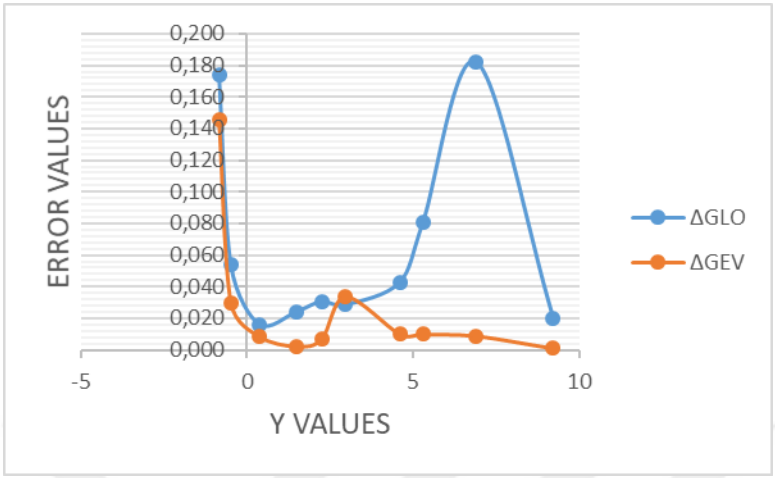

Figure 10.5. Relationship between y and the error values for each of the distributions

Flow values in the first region of Fırat basin can be calculated using the relationship between area and flow 10.4:

$$Q = 0{,}4533A^{0{,}7977} \qquad (10.4)$$

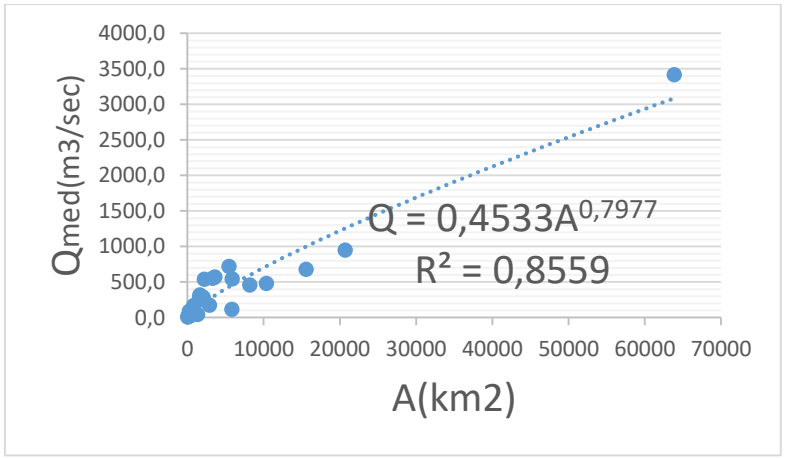

Figure 10.6. Relationship between area and flow for first region of Fırat basin

The optimal distribution for the first Firat basin is the lowest absolute

Z value, GEV has the lowest absolute z value. Using this distribution, regions were simulated 500 times with Monte Carlo simulation method (NSIM = 500) for GEV and GLO distribution. The dimensionless region growth rates, average errors, and errors of these rates bounds are given in Tables 10.19 and 10.20.

Table 10.19. Accuracy measures of the regional growth curve for first region of Firat basin (GEV).

T(Year)	F	q(F)	RMSE	Error bounds		
				95%	5%	Difference
1.11111	0.1	0.283	0.244	0.233	0.329	0.096
1.25	0.2	0.408	0.144	0.357	0.456	0.099
2	0.500	0.782	0.052	0.723	0.822	0.099
5	0.800	1.438	0.029	1.396	1.460	0.064
10	0.900	1.960	0.048	1.882	2.053	0.171
20	0.950	2.525	0.070	2.371	2.744	0.373
100	0.990	4.037	0.114	3.613	4.773	1.16
200	0.995	4.788	0.131	4.210	5.855	1.645
1000	0.999	6.797	0.169	5.742	8.944	3.202
10000	0.9999	10.410	0.218	8.284	15.105	6.821

Table 10.20. Accuracy measures of the regional growth curve for first region of Firat basin (GLO).

T(Year)	F	q(F)	RMSE	Error bounds		
				95%	5%	Difference
1.11111	0.1	0.518	0.685	0.502	0.663	0.161
1.25	0.2	0.653	0.415	0.491	0.685	0.194
2	0.500	0.933	0.034	0.895	0.978	0.083
5	0.800	1.289	0.062	1.222	1.323	0.101
10	0.900	1.540	0.085	1.448	1.591	0.143
20	0.950	1.806	0.102	1.673	1.888	0.215
100	0.990	2.529	0.132	2.238	2.749	0.511
200	0.995	2.903	0.144	2.496	3.208	0.712
1000	0.999	3.962	0.173	3.208	4.594	1.386
10000	0.9999	6.092	0.220	4.496	7.587	3.091

10.2.2 Second Region

Table 10.21Used values in Firat basin for second region

Station name	Duration of observation (Years)	Drainage Area (km^2)	Qmean (m^3/s)
F2167	22	4288	342,8
F2165	29	490	61,1
F2160	21	1020	61,2
F2159	43	1036	121,6
F2131	60	277,6	30
F2115	55	3990,4	515,1
F21-133	17	463,7	57,5
F21-103	22	136,1	27,9
F21-101	23	2047,8	36,8
F21-096	17	725,9	37,3
F21-085	23	266,8	51,2
F21-026	20	128,4	6,2

L-Moment Values were calculated using a plotting-position method usig Excel and the results are shown in Table 10.22

Table 10.22. L-Moment values for second region of Firat basin

Station name	Duration of observation (Year)	Q_{med}	ζ_1	ζ_3	ζ_4	ζ_5	Di
F2167	22	342,85	0,3813	0,3156	0,1748	0,0805	0,49
F2165	29	61,13	0,5232	0,5405	0,4417	0,3596	1,6
F2160	21	61,24	0,4844	0,3254	0,1008	0,0303	1,3
F2159	25	121,57	0,4272	0,1814	0,0572	0,0508	1,09
F2131	60	29,99	0,5060	0,5008	0,3311	0,2018	0,36
F2115	55	515,09	0,3745	0,4746	0,3973	0,2963	2,21
F21-133	17	57,52	0,4808	0,4887	0,3591	0,1750	0,31
F21-103	22	27,92	0,3917	0,1304	0,0231	0,0692	1,29
F21-101	23	36,80	0,4973	0,5629	0,3530	0,1957	0,99
F21-096	17	37,28	0,4008	0,3278	0,1286	0,0590	1,00
F21-085	23	51,21	0,3608	0,2001	0,0576	-0,0031	0,75
F21-026	20	6,16	0,5130	0,5826	0,4122	0,3231	0,60

An incompatibility measure was conducting finding that all values of D for all stations are less than a critical value (Dcr=3). This means that all stations are compatible with each other.

The following results were obtained using the XTest software.

Table 10.23. The results of analysis for second region of Firat basin

***** HETEROGENEITY MEASURES ***** (NUMBER OF SIMULATIONS = 500)	
OBSERVED S.D. OF GROUP L-CV	0,0699
SIM. MEAN OF S.D. OF GROUP L-CV	0,0622
SIM. S.D. OF S.D. OF GROUP L-CV	0,0153
STANDARDIZED TEST VALUE H(1)	-0,09
OBSERVED AVE. OF L-CV / L-SKEW DISTANCE	0,1452
SIM. MEAN OF AVE. L-CV / L-SKEW DISTANCE	0,1089
SIM. S.D. OF AVE. L-CV / L-SKEW DISTANCE	0,0241
STANDARDIZED TEST VALUE H(2)	1,5
OBSERVED AVE. OF L-SKEW/L-KURT DISTANCE	0,1920
SIM. MEAN OF AVE. L-SKEW/L-KURT DISTANCE	0,1372
SIM. S.D. OF AVE. L-SKEW/L-KURT DISTANCE	0,0323
STANDARDIZED TEST VALUE H(3)	1,7

Depending on the previous H values, the region can be considered a homogeneous region. By performing a Z test, the most appropriate distribution of values can be obtained and the results are shown in the Table 10.24.

Table 10.24. Z test's results for second region of Firat basin

DISTRIBUTION	L-Kurtosis	Z
Gen. Logistic	0,212	0,39*
Gen. Extreme Value	0,178	-0,05*
Gen. Normal	0,165	-0,96*
Pearson Type 3	0,142	-2,5
Gen. Pareto	0,097	-1,63*

According to the values of Z, the most appropriate distribution is the one that has $|z|$ value closest to zero value. This indicates that GEV distribution is most appropriate. In general, all distributions that have $|z| < 1.64$ are appropriate.

Regional growth curve is derived based on the simulation results and the index flood procedure. Figure 10.7 shows the curve is fitting very well to his respective set of pooled flood peaks series in the region. Based on the distribution chosen by the goodness-of-fit test, we can see that the respective curve is also fitted statistically.

Table 10.25. Parameter estimates for distributions accepted at the 90% level for second region of Fırat basin

DISTRIBUTION	**ξ (Location Parameter)**	**a (Scale Parameter)**	**K (Shape Parameter)**		
Gen. Logistic	0,725	0,334	-0,407		
Gen. Extreme Value	0,550	0,418	-0,339		
Gen. Normal	0,696	0,576	-0,869		
Gen. Pareto	0,178	0,692	-0,158		
-------	**ξ**	**a**	**B**	**γ**	**δ**
Wakeby	0,116	0,740	4,091	0,553	0,251

Repetitive function of the common regional probability distribution adapted to dimensionless data against certain rotation periods according to these parameters (quantile function) is shown in Table 10.25. The observed values and the flood frequency curves obtained from the distributions given in Table 10.26 were determined graphically (Figure 10.7).

Table 10.26. Quantile function for second region of Firat basin

Y	T	F	GLO	GEV	GNO	GPA	Observed Values
-0,8340	1,1111	0,1000	0,24	0,246	0,251	0,252	0,456
-0,4759	1,25	0,2000	0,371	0,367	0,352	0,336	0,458
0,3665	2	0,5000	0,725	0,714	0,696	0,685	0,642
1,4999	5	0,8000	1,347	1,368	1,410	1,446	1,286
2,2504	10	0,9000	1,911	1,963	2,052	2,100	1,963
2,9702	20	0,9500	2,894	2,964	3,066	3,078	2,800
4,6001	100	0,9900	5,233	5,188	5,041	4,864	5,374
5,2958	200	0,9950	6,986	6,750	6,254	5,913	6,759
6,9073	1000	0,9990	13,57	12,157	9,762	8,840	10,626

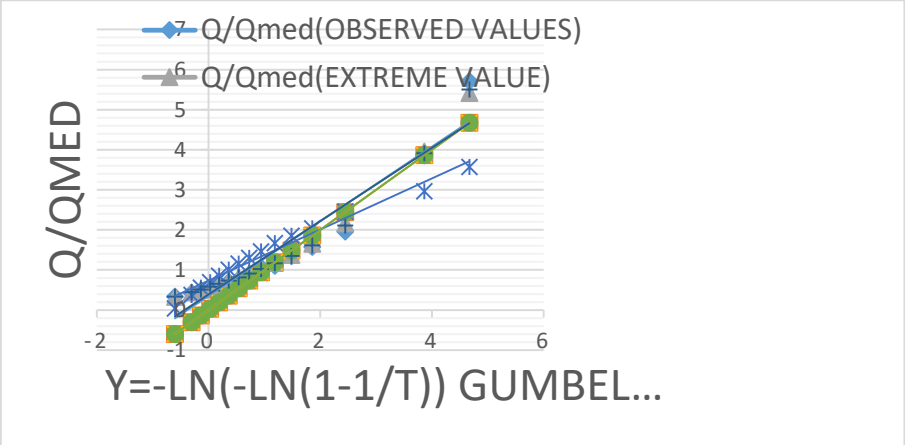

Figure 10.7. Flood frequency curves for second region of Firat basin

flow values in the Dicle basin can be calculated using the extreme value relationship (10.5):

$$q = 0{,}55 - 1{,}233 * \left(1 - (-ln(F)^{-0{,}005})\right) \qquad (10.5)$$

The error value was calculated for each distribution using equation 10.1 and finding the average value of the error values as shown in Table 10.27:

Table 10.27. The Error Values of Each Distribution for First Region of Firat Basin

Y	T	F	GLO	GEV	GNO	GPA	Observed Values	ΔGLO	ΔGEV	ΔGNO	ΔGPA
-0,834	**1,111**	0,1	0,24	0,246	0,251	0,252	0,456	0,474	0,461	0,450	0,447
-0,476	**1,25**	0,2	0,371	0,367	0,352	0,336	0,458	0,190	0,199	0,231	0,266
0,3665	**2**	0,5	0,725	0,714	0,696	0,685	0,642	0,129	0,112	0,084	0,067
1,4999	**5**	0,8	1,347	1,368	1,41	1,446	1,286	0,047	0,064	0,096	0,124
2,2504	**10**	0,9	1,911	1,963	2,052	2,1	1,963	0,026	0,000	0,045	0,070
2,9702	**20**	0,95	2,894	2,964	3,066	3,078	2,8	0,034	0,059	0,095	0,099
4,6001	**100**	0,99	5,233	5,188	5,041	4,864	5,374	0,026	0,035	0,062	0,095
5,2958	**200**	0,995	6,986	6,75	6,254	5,913	6,759	0,034	0,001	0,075	0,125
6,9073	**1000**	0,999	13,57	12,157	9,762	8,84	10,626	0,277	0,144	0,081	0,168
							MEAN	**0,137**	**0,119**	**0,136**	**0,162**

According to the previous results, we find that the most appropriate distribution is the extreme value distribution. This was previously achieved according to the Z test.

The figure 10.8 shows the relationship between Y and the error values for each of the distributions.

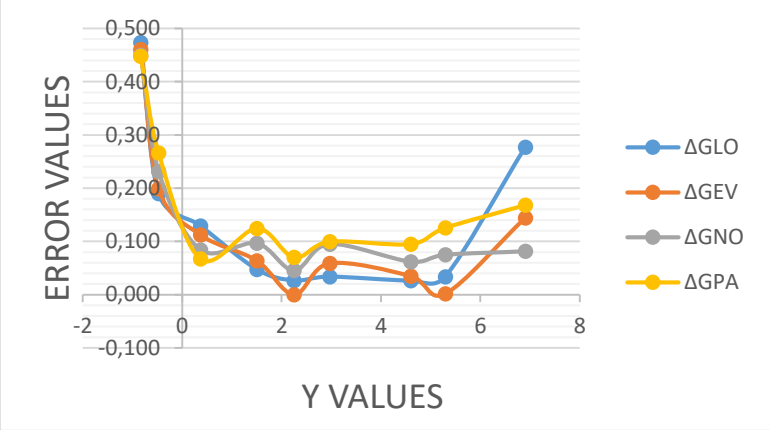

Figure 10.8. Relationship between y and the error values for each of the distributions

Flow values in the Dicle basin can be calculated using the relationship between area and flow 10.6:

$$Q = 0{,}2905A^{0{,}8161} \quad (10.6)$$

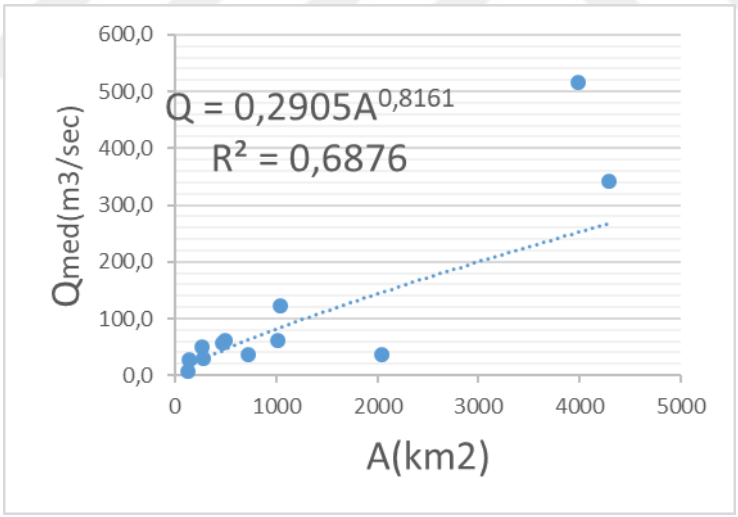

Figure 10.9. Relationship between area and flow for second region of Firat basin

The optimal distribution for the second Fırat basin is the lowest absolute Z value, GEV has the lowest absolute Z value. Using this distribution, regions were simulated 500 times with Monte Carlo simulation method (NSIM = 500) for GNO

and GEV distribution. The dimensionless region growth rates, average errors, and errors of these rates bounds are given in Tables 10.28 and 10.29.

Table 10.28. Accuracy measures of the regional growth curve for second region of Firat basin (GEV).

T(Year)	F	q(F)	RMSE	Error bounds		
				95%	5%	Difference
1.11111	0.1	0.240	0.114	0.062	0.242	0.180
1.25	0.2	0.371	0.488	0.267	0.415	0.148
2	0.500	0.725	0.119	0.628	0.808	0.180
5	0.800	1.347	0.073	1.236	1.369	0.133
10	0.900	1.911	0.100	1.773	1.913	0.14
20	0.950	2.625	0.134	2.369	2.763	0.394
100	0.990	5.233	0.212	4.254	6.440	2.186
200	0.995	6.986	0.248	5.436	9.252	3.816
1000	0.999	13.568	0.340	9.555	21.708	12.153
10000	0.9999	34.826	0.514	8.996	21.564	12.568

Table 10.29. Accuracy measures of the regional growth curve for second region of Firat basin (GNO)

T(Year)	F	q(F)	RMSE	Error bounds		
				95%	5%	Difference
1.11111	0.1	0.251	0.594	0.204	0.315	0.111
1.25	0.2	0.352	0.455	0.235	0.391	0.156
2	0.500	0.696	0.135	0.580	0.792	0.212
5	0.800	1.410	0.059	1.324	1.483	0.159
10	0.900	2.052	0.089	1.944	2.187	0.243
20	0.950	2.802	0.139	2.519	3.230	0.711
100	0.990	5.040	0.201	4.081	6.709	2.628
200	0.995	6.253	0.249	4.866	8.869	4.003
1000	0.999	9.760	0.310	6.897	15.999	9.102
10000	0.9999	16.834	0.399	10.521	33.171	22.65

11. RESULTS

According to the study conducted on the Dicle and Fırat basins, the following results were reached:

- The homogeneity of the hydrological zones determined by DSI and EIEI was tested and determined that the Fırat basin is heterogeneous when considered as a single zone. This basin is divided into two sub-regions, and probability distribution models are applied to all basins.
- GNO distribution was the most appropriate distribution for the Dicle basin. GEV distribution was the most appropriate distribution for the Fırat basin.
- For each basin, the Area-Average flow relationship is proposed. With the help of these equations, the average flow of any point (with or without station) can be calculated.
- Flood frequency curves for each region and equations of these curves have been proposed according to the distribution that best fits the region including regions with no measurement or short recorded stations. After calculating the average flow, the flood flow rate can be calculated with equations due to the possibility of not exceeding any recurrence period.

REFERENCES

Anlı, S. A., Apaydın, H., ve Öztürk, F., 2007. Regional Flood Frequency Estimation For The Göksu River Basin Through L-moments. International Congress on River Basin Management, DSİ, 424-438.

Amit Dubey, 2014 Regional Flood Frequency Analysis Utilizing L-Moments: A Case Study of Narmada Basin. Department of Civil Engineering & Applied Mechanics, S.G.S.I.T.S, Indore, February.

Cunnane, C., 1988. Methods and Merits of Regional Flood Frequency Analysis. Journal of Hydrology, 100: 269-290.

Dalrymple T., 1960. Flood Frequency Methods. U.S. Geol. Survey, Water Supply Paper 1453 A, Washington, 11-51.

DSİ, 1994. Türkiye Akarsu Havzaları Maksimum Akımlar Frekans Analizi (MAFA). Ankara.

Elizabeth M.Shaw, 1994. Hydrology in Practice, Formerly of the Department of Civil Engineering Imperial College of Science, Technology and Medicine, Third Edition.

HAKTANIR, T., 1982. Taşkın Frekans Analizi için Paket Program. DSİ Teknik Bülteni, 53: 48-57.

Hosking, J.R.M., Wallıs, J.R., and Wood, E.F., 1985. Estimation of The Generalized Extreme Value Distribution By The Method of Probability Weighted Moments. Technometrics, 27(3): 251-261.

Hosking, J.R.M., 1986. The Theory of Probability Weighted Moments. Research Rep. RC 12210, 160 pp., IBM Research Division, Yorktown Heights, NY.

Hosking, J.R.M. and Wallis, J.R., 1987. Parameter and Quantile Estimation for The Generalized Pareto Distribution. Technometrics, 29(3): 339-349.

Hosking, J.R.M., and Wallis, J.R., 1988. The Efferct of Intersite Dependence on Regional Flood Frequency Analysis. Water Resources Research, 24, 588-600.

Hosking, J.R.M., 1990. L-Moments:Analysis and Estimation of Distributions Using Lineer Combinations of Order Statistics. J. Royal Statistical Society, 52(2): 105-124.

Hosking, J.R.M., and Wallis, J.R., 1993. Some Statistics Useful in Regional Frequency Analysis. Water Resour. Res., 29(2):271-281, IBM Research Division, Yorktown Heights, New York.

Hosking, J.R.M. and Wallis, J.R., 1997. Regional Frequency Analysis An Approach Based on L-Moments. Cambridge University Press. UK.

Hosking, J.R.M., 2000. FORTRAN Routines for Use with the Method of LMoments. Version 3.03,(http://lib.stat.cmu.edu/general/lmoments).

Hosking, J.R., and Wallis J.R., 1997. Regional frequency analysis-An approach based on Lmoment (Cambridge University Press, Cambridge.

Keshtkar, 2015. Low flow frequency analysis by L-moments method (Case study: Iranian Central Plateau River Basin), Desert Management Department, International Desert Research Center (IDRC), University of Tehran, Tehran 1417763111, Iran.

Muhara, G., 2001. Selection of Flood Frequency Model in Tanzania Using Lmoments and Region of Influence Approach. 2nd WARFSA/WaterNet Symposium: Integrated Water Resources Management: Theory, Practice, Cases; Cape Town, 1-13.

Özcan, Z., 1990. Türkiye Akarsularının Taşkın Pikleri Frekans Analizi. Yüksek Lisans Tezi. İnşaat Mühendisliği Bölümü, Ç.Ü., Adana, 156s.

Peng, S., C. Xi, Q. Si-min, Y. Tao, Z. Zhi-cai, M. Jianliang, 2009. Regional Frequency Analysis of Low Flow Based on L-Moments in Karst Area, Southwest China. Joint International Convention of 8th IAHS Scientific Assembly and 37th IAH Congress, Water: A vital resource under stress – How Science can help, September 6-12, Hyderabad, India.

Bayazıt, M.,Önöz, B., 2008. Taşkın ve Kuraklık Hidrolojisi, University of İstanbul Teknik, Ekim.

Rao R., and Hamed, K.H., 1997. Regional Frequency Analysis of Wabash River Flood Data By L-moments. Journal of Hydrologic Engineering, 169-179.

Seçkin, N., 2009, L-momentlere Dayali Gösterge-Sel Metodu ile Bölgesel Taşkin Frekans Analizi, University of Cukurova.

Şorman, Ü. ve Okur, A., 2000. L-momentler Tekniği Kullanılarak Noktasal ve Bölgesel Frekans Analizinin Uygulanması. İMO Teknik Dergi, 2199-2216.

WMO, 1989. Statistical Distributions For Flood Frequency Analysis. Operational Hydrology Report. No:33, World Meteorological Organization, No:718, Geneva, İsviçre.

Y.H. Lim, 2007. Regional Flood Frequency Analysis of the Red River Basin Using L-moments Approach, Civil Engineering Department, School of Engineering & Mines, University of North Dakota.

CURRICULUM VITAE

After graduating from Jamal Abdulnasser School, he attended Civil Engineering Faculty of Fırat University.

After graduated with the first degree, he started studying master's degree in the Structural Engineering Department at the University of Aleppo, where he worked as a faculty member at the same university between 2014 and 2016. After that he started studying master's degree in the Civil Engineering Department at Cukurova University in 2018, and worked in several companies of steel construction in various fields such as structural studies and engineering management with 3 years of experience in this field.